Research paper
Structural and Optical Properties of Polymer Blend Nanocomposites Based on Poly (vinyl acetate-co-vinyl alcohol)/TiO_2 Nanoparticles

Research Article

ABSTRACT

Titanium dioxide and organic polymer blend poly (vinyl acetate-co-vinyl alcohol) based nanocomposite membranes were prepared and their chemical structure, phase relationship and optical properties investigated. The SEM-EDS analysis reveals TiO_2 to be almost isomorphic ($\geq 99\%$ phase purity) with spherical particles having diameters in the range 25-40nm. The composites were characterized by FTIR, SEM, XRD and UV-vis Spectrophotometry. The FTIR Spectroscopy reveals significant absorptions below 900cm^{-1} to represent Titanium bonds with organic groups and Oxygen while other prominent functional groups above 900cm^{-1} reflect the additivity of polyvinyl alcohol and polyvinyl acetate. It was found that embedding inorganic nanoparticles of TiO_2 into the polymer blend matrix of poly (vinyl acetate-co-vinyl alcohol) allowed for some crystallinity formation and cross-linking of the polymer composites during annealing. The XRD results show more defined peaks assigned to each phase of the composite as the TiO_2 content increases from 1 to 4% weight ratio, thus indicating that Nanoparticle filler remain in the semi-crystalline polymer matrix as a separate crystalline phase, which is in good agreement with the SEM. Finally, the resonant coupling between Ultraviolet-Visible (UV-Vis) light and the collective electronic transitions of polymer nanocomposites are examined using UV-Vis Spectrophotometer. The variation in the percentage absorbance and transmittance over wavelength range 200nm-900nm is also attributed to TiO_2 NPs content (1-4%) in the samples.

Keywords: Polymer blend; TiO_2 Nanoparticles; Polymer Nanocomposites; Chemical structure; UV-Visible light absorber.

1. INTRODUCTION

In the last few years, the prospects for polymer blending have been compared to the alloying of metals because it requires little or no extra capital expenditure compared to the production of new polymers. This leverage has led to extensive use of polymer blends in the polymer industry over the last few years. Also, polymer blending offers the possibility of producing a range of polymeric materials with properties completely different from those of the blend constituents [1]. Blend properties are crucially affected by phase morphology and this in turn

depends upon a number of factors including the choice of parent polymers, compatibilizers, blend composition, moisture content and the method of blend preparation [2,3]. Because of the significant interest in interfacial interaction between inorganic and organic phases (such as variety of polymer and their blend derivatives) as well as size-dependent phenomena of nanoscale particles, polymer blend nanocomposites are capable of dramatically improving numerous favorable properties without losing the inherent good properties of the polymer phases such as ductility, optical transparency etc. these advantages are never achieved in the conventional polymer composites. In addition, property enhancements in polymer nanocomposites are achieved at a very low loading (<5 wt %) of inorganic nanoparticles while the conventional polymer composites usually require much loading of the order of 25-40 wt % [4].

In contrast to the traditional dyes, inorganic semiconductive nanocrystals have more resistant to chemical attacks and low degradation with higher photobleaching, broader excitation wavelength range, narrower and tunable emission spectra [5,6,7,8]. This influence has attracted an enormous research effort leading to a myriad of potential applications in engineering, medicine, biology, electronics and allied industries. Their optical properties have been the center of attraction due to strong size-dependent quantum confinement effect associated with inorganic semiconductive nanocrystals. For the development of novel nanodevices such as electronics and optical devices, various stabilizers (surfactants, polymers or coupling agents) have been employed to modify the surface functionalities of the nanocrystals [9,10], as these nanocrystals are seldom prepared without aggregation. A great deal of attention has been focused on TiO_2 in contrast to other semiconducting materials, because of its low cost, non-toxicity, chemical stability, resistance to photocorrosion, high photocatalytic activity and high refractive index [11,12]. In the last decade, most studies are mainly focused on the dispersion of nanocrystalline TiO_2 powder for photocatalysis compared to TiO_2 thin films due to its higher photocatalytic activity [13]. It is an established fact that a mixture of anatase TiO_2 and a small percentage of rutile TiO_2 give optimal photocatalytic efficiency as the anatase phase has a wider band gap of 3.20 eV [14].

Polymer nanocomposites represent a merger between traditional organic and nanosized inorganic materials, resulting in compositions that are truly hybrid. The key to forming such novel materials is adequate understanding and manipulation of the guest-host chemistry, occurring between the polymer and the nanoparticles, in order to obtain a homogenous dispersion and a good contact between polymer and added particle surfaces [15]. Generally, the resultant nanocomposites display enhanced favorable properties such as conductivity, toughness, optical activity, catalytic activity, chemical selectivity etc [16]. These attributes have led to the growing interest and uses in various fields such as military equipments, safety and protective garments, automotive, aerospace, electronic and optical devices. A lot of research works exploiting these aforementioned properties have been carried out for possible applications including flame retardancy, chemical resistance, UV resistance, electrical conductivity, environmental stability, water repellency, magnetic field resistance, radar absorption etc [17, 18, 19, 20, 21].

In this paper, we report the development of Poly (vinyl acetate-co-vinyl alcohol)/TiO_2 nanocomposites achieved via a two-stage synthetic route and the relationship between structural and optical properties of the resulting hybrid Poly(vinyl acetate-co-vinyl alcohol)/TiO_2 nanocomposites employing Fourier Transform Infrared (FTIR) spectroscopy, Scanning Electron Microscopy (SEM), X-Ray Diffraction (XRD) analysis and UV-Visible Spectrophotometry.

2. MATERIAL AND METHODS

Poly (vinyl acetate-co-vinyl alcohol)/TiO_2 nanocomposites were produced via a two-stage reaction involving the synthesis of TiO_2 Nanoparticles (Nps) from titanium (IV) chloride {$TiCl_4$, BDH Limited Poole, England} employing hydrothermal technique and subsequent mixing of modified TiO_2 Nps with Poly(vinyl acetate-co-vinyl alcohol) dissolved in toluene via one-pot reaction. Surface morphology of the synthesized TiO_2 nanoparticles was observed using EVOI MA10 (ZEISS) multipurpose scanning electron microscope operating at 20kV employing secondary electron signals. Four samples of Poly (vinyl acetate-co-vinyl alcohol)/TiO_2 nanocomposites containing 1-4% of TiO_2 Nps were produced by solution casting into Petri dishes. The samples were oven dried at temperature lower than the melting point of the polymer blend for 12hrs and subsequently flat and uniform thin samples were obtained. The FTIR spectra of all the component reagents, polymer blend and the prepared nanocomposite samples were obtained using SHIMADZU FTIR-8400S Spectrophotometre in transmission mode without KBr. The spectra were recorded in the frequency range from 400 to 4600 cm^{-1}, after 25 scans, with resolution of $2cm^{-1}$. The positions and intensities of the IR bands were processed with Spectral Analysis software.

Surface morphologies of Poly (vinyl acetate-co-vinyl alcohol)/TiO_2 nanocomposites were observed using EVOI MA10 (ZEISS) multipurpose scanning electron microscope operating at 20kV employing secondary electron signals at a magnification of 200X and the particle size distribution was obtained using imaging software (Image-J). The crystallinity of polymer blend/TiO_2 nanocomposites was observed using X-Ray Diffractometre (Phillips X'pert Pro X-Ray Diffractometre) employing a 1.54060Å copper X-ray source. The samples were scanned from $2\theta = 5^o$-80^o using a step size of 0.06^o. The percentage crystallinity (X_c) was calculated following the procedure proposed by [22], with the Scientific Graphing and Data Analysis Software (Origin 8.0), using the following equation: $X_c = \frac{A_c}{A_c + A_a}$ where X_c, (percentage crystallinity), is the ratio of crystalline peak area (A_c) to the sum of the crystalline peak area (A_c) and amorphous peak area (A_a). Finally, the absorption/filtering property of the polymer blend /TiO_2 nanocomposites was studied in the ultraviolet (UV) radiation wavelength range of 200nm-400nm and visible radiation wavelength range of 400nm-900nm using JENWAY 6405 UV-visible Spectrophotometre.

3. RESULTS AND DISCUSSION

The image presented in figure 1 together with the corresponding EDS spectra obtained using characteristic x-rays emitted by TiO_2 nanoparticles was observed at a magnification of 83.04kX. The uniform contrast in the image revealed TiO_2 to be almost isomorphic. Nevertheless, Oxygen and Nitrogen occur with minor concentrations as impurities thereby making Ti the dominant element with concentration of about 99.5% as depicted in the EDS spectra (fig 1b). The morphology of TiO_2 nanoparticles is such that the particles are closely packed and spherical in shape. The average diameter of the particles is in the range of 25-40nm reflecting that TiO_2 nanoparticles are transparent and suitable filler for polymer composite applications.

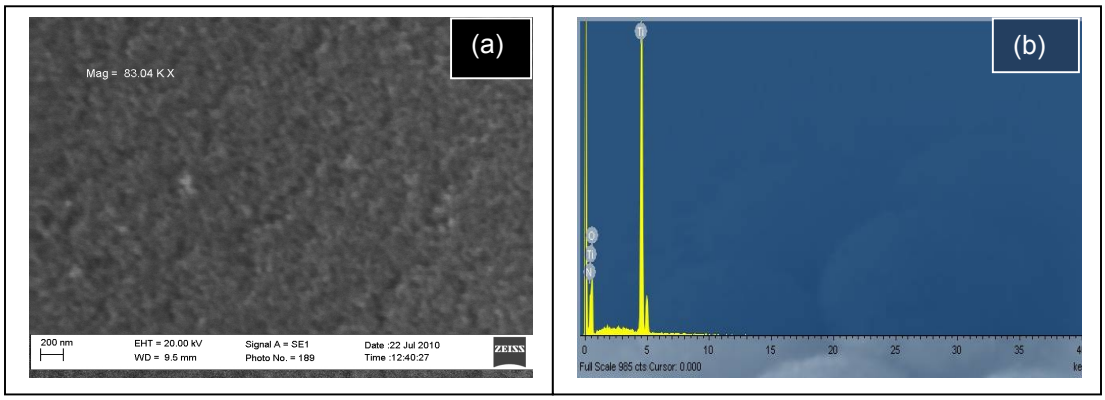

Figure 1: Microstructure and elemental composition of TiO2 Nps: (a) SEM image of TiO_2 Nps (b) EDS spectra of TiO_2 Nps.

It is an established fact that the fundamental vibrations of solids (finger prints) are localized in the low frequency region (<1200cm^{-1}) of the midrange (400-4000cm^{-1}) of the infrared (IR) spectrum. Also, as reported by [23], the Ti-O bond is clearly located in the range from 400-900cm^{-1}. In this work, the significant absorptions observed below 900cm^{-1} represent Ti bonds with vinyl groups, secondary alcohols, carbonyl groups and oxygen.

The spectra for the functionalized TiO_2 nanoparticles, poly (vinyl alcohol), poly (vinyl acetate), polymer blend [polyvinyl (acetate + vinyl alcohol)] and the functionalized TiO_2 are given in figure 2 (a-d) below. The prominent functional groups in poly (vinyl alcohol), poly (vinyl acetate) and their blend are OH stretching vibrations, CH_2 stretching and bending vibrations, CH_3 bending vibrations, C-O-C vibration in esters, vC=O stretching vibration, C-OH stretching vibrations, CH bending and C=O stretching vibration.

The observed spectra of the polymer-blend/TiO_2 nanocomposites reveal the additivity of the spectra of polyvinyl alcohol and poly vinyl acetate with the modified TiO_2 NPs. In figures 3(a) and 3(b), most of the functional groups peculiar to the component reagents were observed but in figures 3(c) and 3(d), chemical reactions between the component reagents and the increase in the concentration of the functionalized TiO_2 nanoparticles from 2%-4% are responsible for the extinction of the functional groups as a result of oxidation and hydrolysis.

From figure 3(a-d), it can equally be deduced that the OH stretching vibrations of the intermolecular hydrogen bonding occurring in the range 3427.62cm^{-1}-3483.56cm^{-1} is basically due to the adsorbed H-O-H. Organics (methylene groups) are also represented by the v_{as}-CH_2 asymmetrical stretching vibrations in ranges slightly above 2910cm^{-1}. The CH stretching vibrations with coexisting terminal triple bonds resulting from remnant alkynes occur in the range 2067.76cm^{-1}-2145.88cm^{-1}. All the changes observed in the vibration frequency of vC=O in the blend indicates that the incorporation of the nanofillers (TiO_2) has great influence on the vibration frequency of vC=O. Furthermore, conjugation with CH_3 (phenyl groups) results in an increase in bond length of C=O thereby creating functional sites on the surface of the polymer blend. The C-O-C vibrations in esters occurring in the frequency ranges 949.01cm^{-1}-950.94cm^{-1} and 1284.63cm^{-1}-1293.31cm^{-1} represent the possible combination of acetate and alcohol groups. Finally, the functional groups appearing

in the range 383.85cm^{-1}-491.66cm^{-1} represent Ti-O bonds of the functionalized TiO_2 nanoparticles.

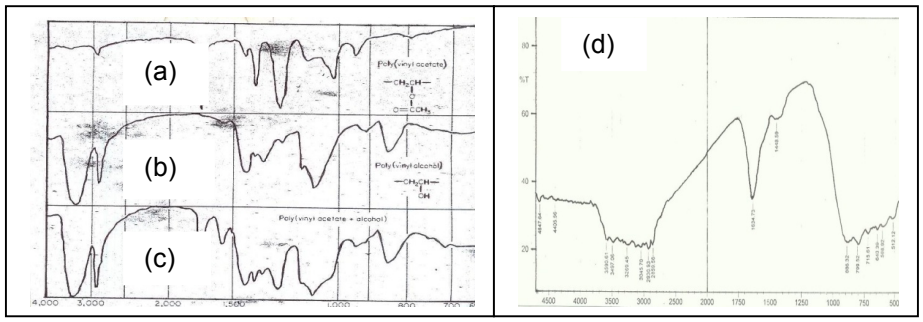

Figure 2: FTIR Spectra of (a) Poly (vinyl alcohol), (b) Poly (vinyl acetate), (c) Polymer Blend and (d) Functionalized TiO_2 Nps.

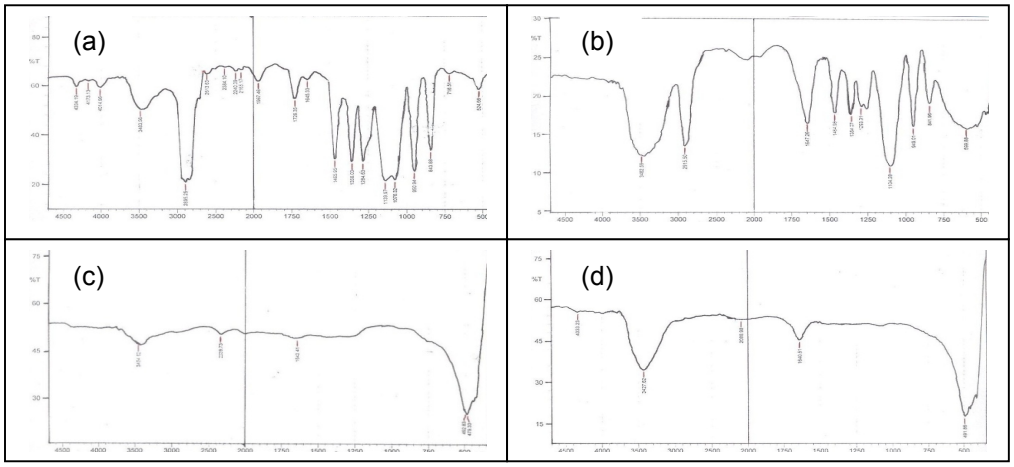

Figure 3: FTIR Spectra of Polymer blend/ TiO_2 Nanocomposites containing: (a) 1% of TiO_2 Nps (b) 2% of TiO_2 Nps (c) 3% of TiO_2 Nps and (d) 4% of TiO_2 Nps.

The uneven baseline in the XRD patterns seen in figure 4 (a-d) for all the samples is due to the large amount of amorphous polymer content. The addition of TiO_2 nanoparticles to the polymer blends improved the crystallinity of the composites. The diffraction peaks in the range $2\theta = 15^o$-20^o can be linked to crystalline behaviour of the polymer blends. The peaks at $2\theta = 19.66^o$, 19.84^o, 20.34^o, and 20.49^o with d-spacings d = 4.5154Á, 4.4742Á, 4.3642Á and 4.3325Á indicate the presence of crystalline structure of PVA, consistent with the works of [24, 25]. Furthermore, the XRD patterns of polymer blend/TiO_2 nanocomposites reveal the presence of TiO_2 phase but few peaks representing TiO_2 phase have been shifted slightly to lower 2θ values ($2\theta = 21.9147^o$, 22.1288^o, 22.3682^o, 22.4479^o, 22.77578^o, 22.8024^o and

22.9986°) due to slight expansion of TiO_2 crystal structure as a result of surface modification and bonding with the polymer blend matrix. This is also consistent with the results presented in some literatures [26, 27]. The average crystallite size corresponding to structural order of the pattern determined from integral breadth of the peaks according to Scherrer's equation [28] have values ranging from 1687.93±290nm to 4589.04±130nm. The percentage crystallinity values of the polymer blend/TiO_2 nanocomposites following the procedure proposed by [22] range from 56.9 ± 0.2% to 67.6 ± 0.7%. The sample with 4% TiO_2 content displayed higher percentage crystallinity compared to other samples.

The microstructure of the polymer blend/TiO_2 nanocomposites reveals two distinct phases comprising of lighter modified TiO_2 nanoparticles and dark bulk polymer blend matrix. The lighter modified TiO_2 nanoparticles are evenly dispersed over the dark bulk polymer matrix with spherical shapes and the concentration increased with increasing content of the modified TiO_2 NPs (1%-4%) as depicted in figure 5(a-d). The contrast observed in the SEM images [figure 5(a-d)] arises from atomic number difference, since phases within a material are dependent upon back scattered electron yield and the corresponding atomic number of atoms present within different phases. As such, the modified TiO_2 nanoparticles appear lighter compared to the bulk polymer blend matrix because the atoms present in TiO_2 phase have higher atomic numbers and higher back scattered electron yield. The average particle diameters of the polymer-blend/TiO_2 nanocomposites as determined from SEM images using imaging software (Image J) range from 119±5μm to 179±4μm.

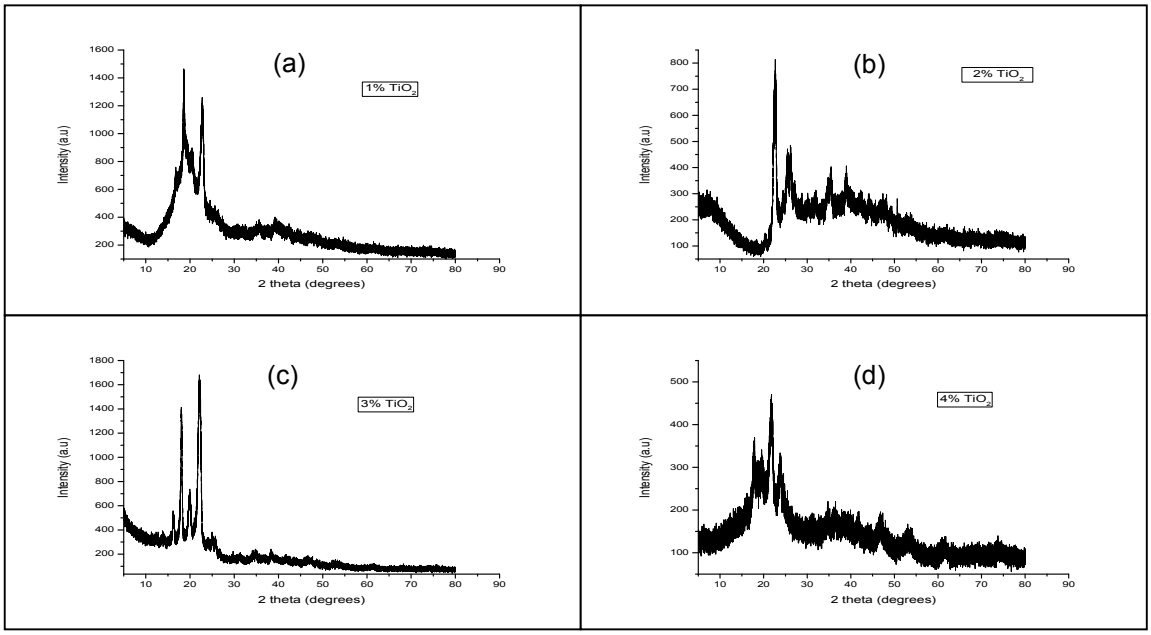

Figure 4: X-ray Diffraction Patterns of Polymer Blend/TiO_2 Nanocomposites containing (a) 1% of TiO_2, (b) 2% of TiO_2,(c) 3% of TiO_2 and (d) 4% of TiO_2 .

(electronic transitions/excitations) of the polymer nanocomposites. The interaction of the UV-visible light with the polymer nanocomposites possibly will give rise to polarization of the nanocomposite matrix, which in turn can be seen as variation in the magnitude of absorption/transmission with respect to changes in wavelengths (i.e. 200-900nm) when examined using UV-vis spectrophotometre. In addition to this, anisotropy of the

nanocomposite matrix resulting from addition of TiO_2 nanoparticles gave rise to varied properties as a result of slight structural modifications. These structural modifications have been studied using FTIR, XRD and SEM. The slight variation in the percentage absorbance over wavelength range (i.e. 200-900nm) is attributed to the TiO_2 nanoparticles content (1-4%) in each sample.

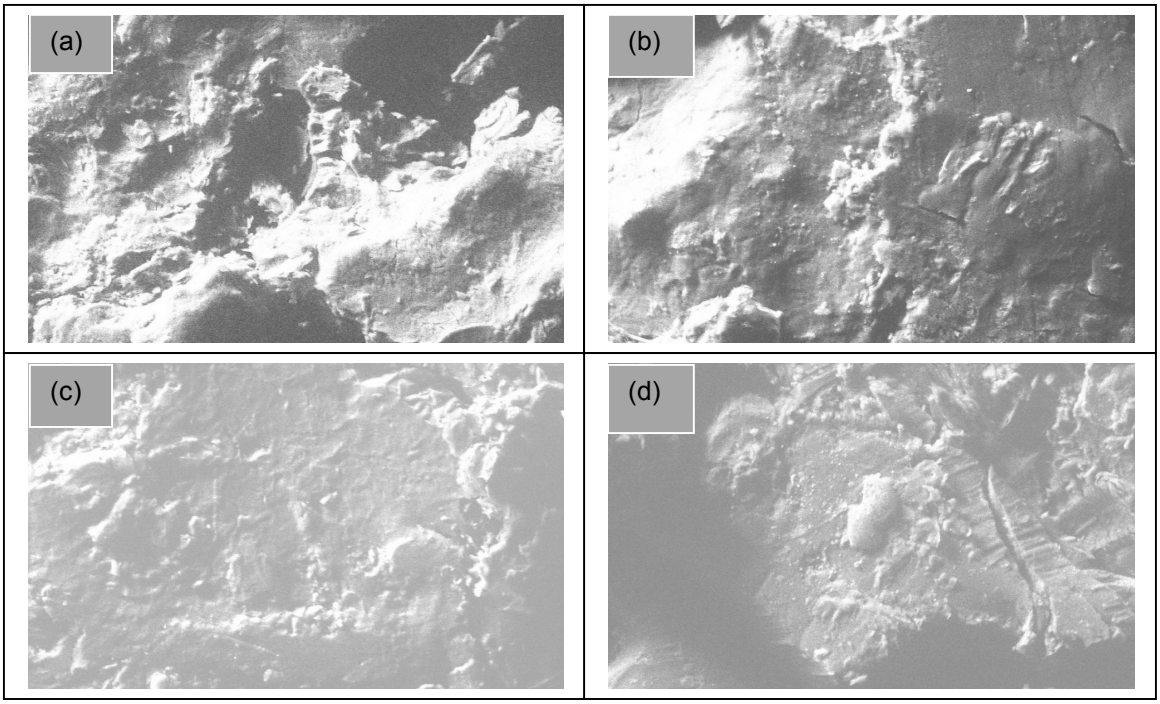

Figure 5: SEM Images of Polymer Blend/TiO_2 Nanocomposites containing: (a) 1% of TiO_2, (b) 2% of TiO_2,(c) 3% of TiO_2 and (d) 4% of TiO_2

The UV-Vis spectra of polymer blend/TiO_2 nanocomposites are given in figure 6(a-d) below. The plot for polymer blend/TiO_2 sample (containing 1 wt % of nanoparticles) is presented in figure 6(a). The sample filters at the onset of ultraviolet radiation wavelength through 295nm above which it absorbs significantly and rapidly until maximum absorbance of 1.385% is recorded at a wavelength of 390nm. Slightly above the visible range, there is little decline in absorbance but appreciates reasonably through the whole range with maximum recorded at a wavelength of 1.663nm.The sample has displayed excellent property of being an ultraviolet radiation filter at low wavelengths (<300nm) and absorber at higher wavelengths (300-400nm) of the UV range in addition to being an excellent visible absorber. Figure 6(b) portrays the behaviour for polymer blend sample containing 2 wt % of TiO_2 nanofillers. The spectrum shows absolute transparency from the onset of ultraviolet radiation wavelength range through a visible wavelength of 515nm. A much significant absorbance of 2.997%, the maximum, is recorded slightly above that (i.e. at 520nm) from which the absorbance decreases very slightly with a minimum of 2.708% at 800nm. This material is an excellent UV filter and a very good visible radiation absorber.

A similar behaviour to the polymer blend samples described above is observed in both the remaining blend samples (with 3 wt % and 4 wt % of TiO_2 nanofillers respectively) as depicted in figures 6(c) and 6(d). However, there are slight shifts in the onsets of absorption, with the sample containing 3 wt % of TiO_2 having onset at a wavelength of 590nm corresponding to maximum absorbance of 2.983% and that containing 4 wt % of TiO_2 having onset at 550nm corresponding to maximum absorbance of 2.982% as well. The minimum absorbance for these samples are recorded at 795nm (2.835%) and at 780nm (2.729%) respectively.

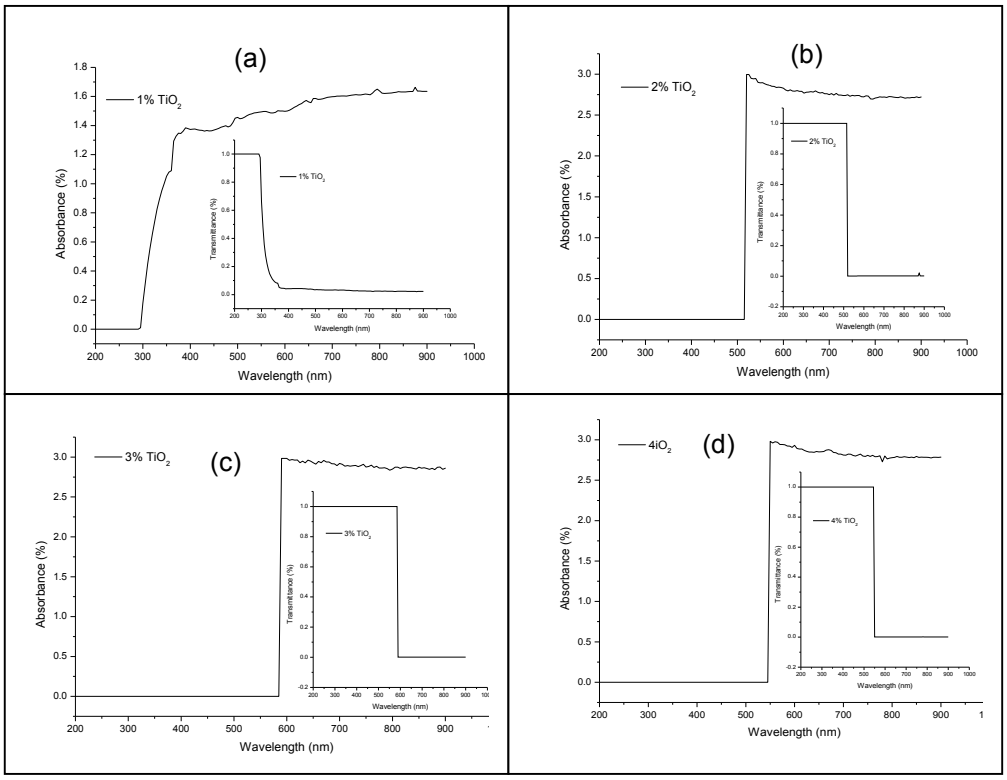

Figure 6: UV-vis spectra of Polymer-Blend/TiO_2 Nanocomposites containing: (a) 1% of TiO_2, (b) 2% of TiO_2, (c) 3% of TiO_2 and (d) 4% of TiO_2.

4. CONCLUSION

The development of the polymer blend nanocomposites was realized by surface modification of TiO_2 Nps in order to create functional sites and improve dispersion of nanoparticles in the polymer blend matrices. FTIR spectroscopy proved the existence of covalent chemical bonding between the polymer chains and inorganic phase in the polymer blend nanocomposites. Thus, revealing significant absorptions below 900cm^{-1} to represent titanium bonds with organic groups and oxygen while other prominent functional groups above

900cm^{-1} reflect the additivity of polyvinyl acetate and polyvinyl alcohol. X-ray diffraction analysis of the polymer blend nanocomposites revealed an increase in the percentage crystallinity from 56.9 ± 0.2% to 67.6 ± 0.7% for the polymer-blend nanocomposites as TiO_2 nanoparticles content increases from 1% to 4%. Observations from SEM analysis showed that the dispersion of TiO_2 nanoparticles in the polymer matrix was relatively uniform with particles having good adhesion with polymer domains. Investigation with UV-visible spectrophotometre revealed that the dispersion of TiO_2 nanoparticles improved the optical properties of the polymer blends. The fact that nanocomposites displayed some level of transparency at lower wavelengths indicates that the nanoparticles are not agglomerated. In addition, strong UV absorption in some of the nanocomposite samples was observed because of the incorporated TiO_2 particles. In fact, with the exception of sample with 1% content of nanoparticles, all the samples transmit UV radiation and absorb visible radiation at wavelengths of 520nm, 590nm and 550nm respectively. Thus the developed polymer blend nanocomposites could act as an efficient optically transparent UV filter and visible radiation absorber.

ACKNOWLEDGEMENTS

We thank Physics Advanced Laboratory, Sheda Science and Technology Complex, Abuja, Nigeria and National Research Institute for Chemical Technology, Zaria, Nigeria for technical assistance during the experimental characterization.

COMPETING INTERESTS

Authors have declared that no competing interests exist.

AUTHORS' CONTRIBUTIONS

This work was carried out in collaboration between all authors. Authors TOA and POA designed the study. Author TOA wrote the protocol and wrote the first draft while, author TOA and author IA carried out the experimental work and analyses. Author TOA and author IA managed the literature searches. All authors read and approved the final manuscript.

REFERENCES

1. Wanchoo RK, Sharma PK. Viscometric Study on the Compatibility of some Water Soluble Polymer-Polymer Mixtures. Euro. Polym. J. 2003: 39: 1481-82.

2. Dyson RW. Engineering Polymers. Chapman and Hall, New York. 1990: 20-28

3. Chuu MS, Meyers RR. Effect of Moisture content on the dielectric behaviour of Poly (vinyl acetate)-Natural Rubber blend. J Appl Polym Sci. 1987: 34 (4):1447

4. Saujanya C, Radhakrishna S. Polymer Nanocomposites, J. of Polym. Sci. 2001: 42: 6723-6731.

5. Riegler J, Ditengou F, Palme K, Nann T. Blue Shift of CdSe/ZnS Nanocrystals-Labels upon DNA-Hybridization. J. Nanobiotechnol. 2008: 6(1): 7.

6. Bruchez Jr. M, Moronne M, Gin P, Weiss S, Alivisatos AP. Semiconductor Nanocrystals as Fluoresecent Biological labels. Science. 1998: 281(5385):2013–2016.

7. Chan WCW, Nie S. Quantum Dot Bioconjugates for Ultrasensitive Nonisotopic Detection Science. 1998: 281(5385): 2016–2018.

8. Jaiswal J, Mattoussi H, Mauro J, Simon S. Long-term multiple Color Imaging of Live Cells Using Quantum Dot Bioconjugates. Nat. Biotechnol. 2003: 21(1): 47–51.

9. Patra MK, Manoth M, Singh VK, Gowd GS, Choudhry VS, Vadera SR, Kumar N. Synthesis of Stable Dispersion of ZnO Quantum Dots in Aqeous Medium Showing visible Emission from Bluish-Green to Yellow. J. Lumin. 2009: 129 (3):320–324.

10. Guo Z, Kumar C, Henry LL, Domes EE, Hormes J, Podlaha EJ. Displacement Synthesis of Cu Shells Surrounding Co Nanoparticles. J. Electrochem. Soc. 2005: 152(1): D1–D5.

11. Legrini O, Oliveros E, Braun AM, Photochemical Processes for Water Treatment. Chem. Rev. 1993: 93(2): 671-698.

12. Sugimoto T, Zhou X, Muramatsu A. Synthesis of Uniform Anatase TiO_2 Nanoparticles by Gel-Sol Method: 3. Formation Process & Size Control. J. Colloid Interface Sci. 2003: 259(1): 43-52.

13. Jiaguo Y, Jimmy CYU, Cheng B, Zhao X. Photocatalytic Activity & Characterization of the Sol-Gel Derived Pb-Doped TiO_2 Thin-films J. Sol-Gel Sci. Tech. 2002: 24(1) 39-48.

14. Bouras P, Stathatos E, Lianos P. Pure versus Metal-ion-doped Nanocrystalline Titania for Photocatalysis. Appl. Catal. B:Environ. 2007: 73(1-2): 51-59.

15.Lagashetty A, Venkataramen I. Polymer Nanocomposites. John Wiley and sons. 2005.

16.Garcia C, Maria M, Dela L. Polymer-Inorganic Nanocomposites: Influence of Colloidal Silica, A PhD thesis submitted to the university of Twente, Netherlands. 2004.

17.Mohan S, Lauren NC, Surya SG, Karen IW. Melt Intercalation of Polystyrene in Layered Silicates, J. of Polym. Sci.: part B: Polym. Physics. 1996: 34: 1433-1449.

18. Lee SS, Lee CS, Kim MH, Kwak SY, Park M, Lim S, Choe CR, Kim J. Specific Interaction Governing the Melt Intercalation of Clay with Poly(styrene-co-acrylonitrile) Copolymers. J. of Polym. Sci.: part B: Polym. Physics. 2001: 39: 2430-2435.

19. Pegoretti A, Dorigato A, Penati A. A Tensile Mechanical Response of Polyethylene-Clay Nanocomposites. Express Polymer Letters. 2007: 1(3): 123-131.

20. Tolstov AL, Matyushov VF, Klymchok, DO. Synthesis and Characterization of Hybrid Cured Poly (ether-urethane) Acrylate/Titania Microcomposites Formed from Tetraalkoxytitanate Precursors, Express Polymer Letters. 2008: 2(6) 449-459.

21. Manias E, Zhang J, Huh JY. Polyethylene Nanocomposite Heat Sealants with a Versatile Peelable Character, Macromol. Rapid Commun. 2009: 30: 17-23.

22. Eichhorn S J, Young RJ. The Young's modulus of Microcrystalline cellulose. Cellulose. 2001: 8: 197-207.

23. Morterra C, Magnacca G. A case Study: Surface Chemistry & Structure of Catalytic Aluminas as Studied by Vibrational Spectroscopy of Adsorbed species" Catal.Today. 1996: 27: (3-4): 497-532.

24. G'eminarda JC, Bonraya DH. Thermal Conductivity Associated with a Bead-Bead Content Decorated by a Liquid Bridge; An Experimental Study Based on the Response of a Chain Subjected to Thermal Cycles. Gayvallet Eur, Phys. 2005: 48: 509-517.

25. Lee GW, Park M, Kim J, Lee JI, Yoon HG. Enhanced thermal conductivity of polymer Composites filled with hybrid filler. Composites Part A: Applied Science and Manufacturing. 2006: 37: 727–734.

26. Shuqiang J, Hongmin Z. Electrolysis of Ti_2CO Solid Solution Prepared by TiC & TiO_2, Journal of Alloys & Compounds. 2007: 2007: 438: 243-246.

27. Yang Z, Choi D, Kerisit S, Rosso KM, Wang D, Zhang Z, Graffi G, Liu J. Nanostructures and Lithium Electrochemical Reactivity of Lithium titanates and Titanium oxides: A Review. Journal of Power Sources. 2009: 192(2): 588-598.

28. Patterson AL. The Scherrer formula for X-ray particle size determination. Physical Review. 1939: 56(10): 978-982.